Received: 23 May 2019 | Accepted: 31 May 2019
DOI: 10.1002/pip.3171

ACCELERATED PUBLICATION

WILEY PROGRESS IN PHOTOVOLTAICS

Solar cell efficiency tables (version 54)

Martin A. Green[1] | Ewan D. Dunlop[2] | Dean H. Levi[3] | Jochen Hohl-Ebinger[4] | Masahiro Yoshita[5] | Anita W.Y. Ho-Baillie[1]

[1] School of Photovoltaic and Renewable Energy Engineering, Australian Centre for Advanced Photovoltaics, University of New South Wales, Sydney 2052, Australia

[2] Directorate C—Energy, Transport and Climate, European Commission—Joint Research Centre, Via E. Fermi 2749, IT-21027Ispra (VA), Italy

[3] National Renewable Energy Laboratory, 15013 Denver West Parkway, Golden, CO 80401, USA

[4] Department of Characterisation and Simulation/CalLab Cells, Fraunhofer-Institute for Solar Energy Systems, Heidenhofstr. 2, D-79110 Freiburg, Germany

[5] Research Center for Photovoltaics (RCPV), National Institute of Advanced Industrial Science and Technology (AIST), Central 2, Umezono 1-1-1, Tsukuba, Ibaraki 305-8568, Japan

Correspondence
Martin A. Green, School of Photovoltaic and Renewable Energy Engineering, University of New South Wales, Sydney 2052, Australia.
Email: m.green@unsw.edu.au

Funding information
Japanese New Energy and Industrial Technology Development Organisation (NEDO); US Department of Energy, Grant/Award Number: DE-AC36-08-GO28308; Australian Renewable Energy Agency (ARENA)

Abstract
Consolidated tables showing an extensive listing of the highest independently confirmed efficiencies for solar cells and modules are presented. Guidelines for inclusion of results into these tables are outlined, and new entries since January 2019 are reviewed.

KEYWORDS
energy conversion efficiency, photovoltaic efficiency, solar cell efficiency

1 | INTRODUCTION

Since January 1993, "*Progress in Photovoltaics*" has published six monthly listings of the highest confirmed efficiencies for a range of photovoltaic cell and module technologies.[1-3] By providing guidelines for inclusion of results into these tables, this not only provides an authoritative summary of the current state-of-the-art but also encourages researchers to seek independent confirmation of results and to report results on a standardised basis. In Version 33 of these tables,[3] results were updated to the new internationally accepted reference spectrum (International Electrotechnical Commission IEC 60904-3, Ed. 2, 2008).

The most important criterion for inclusion of results into the tables is that they must have been independently measured by a recognised test centre listed elsewhere.[2] A distinction is made between three different eligible definitions of cell area: total area, aperture area, and designated illumination area, as also defined elsewhere[2] (note that, if masking is used, masks must have a simple aperture geometry, such as square, rectangular, or circular). "Active area" efficiencies are not included. There are also certain minimum values of the area sought for the different device types (above 0.05 cm^2 for a concentrator cell, 1 cm^2 for a one-sun cell, 800 cm^2 for a module, and 200 cm^2 for a "submodule").

Results are reported for cells and modules made from different semiconductors and for subcategories within each semiconductor grouping (eg, crystalline, polycrystalline, and thin film). From Version 36 onwards, spectral response information is included (when possible) in the form of a plot of the external quantum efficiency (EQE) versus wavelength, either as absolute values or normalised to the peak measured value. Current-voltage (IV) curves have also been included where possible from Version 38 onwards. A graphical summary of progress over the first 25 years during which the tables have been published has been included in Version 51.[2]

Highest confirmed "one-sun" cell and module results are reported in Tables 1–4. Any changes in the tables from those previously published[1] are set in bold type. In most cases, a literature reference is provided that describes either the result reported, or a similar result (readers identifying improved references are welcome to submit to the lead author). Table 1 summarises the best-reported measurements for "one-sun" (non-concentrator) single-junction cells and submodules.

Table 2 contains what might be described as "notable exceptions" for "one-sun" single-junction cells and submodules in the above category. While not conforming to the requirements to be recognised as a class record, the devices in Table 2 have notable characteristics that will be of interest to sections of the photovoltaic community, with

TABLE 1 Confirmed single-junction terrestrial cell and submodule efficiencies measured under the global AM1.5 spectrum (1000 W/m^2) at 25°C (IEC 60904-3: 2008, ASTM G-173-03 global)

Classification	Efficiency, %	Area, cm^2	V_{oc}, V	J_{sc}, mA/cm^2	Fill Factor, %	Test Centre (Date)	Description
Silicon							
Si (crystalline cell)	26.7 ± 0.5	79.0 (da)	0.738	42.65[a]	84.9	AIST (3/17)	Kaneka, n-type rear IBC[4]
Si (multicrystalline cell)	22.3 ± 0.4[b]	3.923 (ap)	0.6742	41.08[c]	80.5	FhG-ISE (8/17)	Fraunhofer ISE, n-type[5]
Si (thin transfer submodule)	21.2 ± 0.4	239.7 (ap)	0.687[d]	38.50[d,e]	80.3	NREL (4/14)	Solexel (35 μm thick)[6]
Si (thin film minimodule)	10.5 ± 0.3	94.0 (ap)	0.492[d]	29.7[d,f]	72.1	FhG-ISE (8/07)	CSG Solar (<2 μm on glass)[7]
III-V cells							
GaAs (thin film cell)	29.1 ± 0.6	0.998 (ap)	1.1272	29.78[g]	86.7	FhG-ISE (10/18)	Alta devices[8]
GaAs (multicrystalline)	18.4 ± 0.5	4.011 (t)	0.994	23.2	79.7	NREL (11/95)	RTI, Ge substrate[9]
InP (crystalline cell)	24.2 ± 0.5[b]	1.008 (ap)	0.939	31.15[a]	82.6	NREL (3/13)	NREL[10]
Thin film chalcogenide							
CIGS (cell) (Cd-free)	**23.35 ± 0.5**	**1.043 (da)**	**0.734**	**39.58**[h]	**80.4**	**AIST (11/18)**	**Solar Frontier**[11]
CdTe (cell)	21.0 ± 0.4	1.0623 (ap)	0.8759	30.25[e]	79.4	Newport (8/14)	First Solar, on glass[12]
CZTSSe (cell)	11.3 ± 0.3	1.1761 (da)	0.5333	33.57[g]	63.0	Newport (10/18)	DGIST, Korea[13]
CZTS (cell)	10.0 ± 0.2	1.113 (da)	0.7083	21.77[a]	65.1	NREL (3/17)	UNSW[14]
Amorphous/microcrystalline							
Si (amorphous cell)	10.2 ± 0.3[i,b]	1.001 (da)	0.896	16.36[e]	69.8	AIST (7/14)	AIST[15]
Si (microcrystalline cell)	11.9 ± 0.3[b]	1.044 (da)	0.550	29.72[a]	75.0	AIST (2/17)	AIST[16]
Perovskite							
Perovskite (cell)	20.9 ± 0.7[i,k]	0.991 (da)	1.125	24.92[c]	74.5	Newport (7/17)	KRICT[17]
Perovskite (minimodule)	17.25 ± 0.6[j,l]	17.277 (da)	1.070[d]	20.66[d,m]	78.1	Newport (5/18)	Microquanta, 7 serial cells[18]
Perovskite (submodule)	11.7 ± 0.4[j]	703 (da)	1.073[d]	14.36[d,m]	75.8	AIST (3/18)	Toshiba, 44 serial cells[19]
Dye sensitised							
Dye (cell)	11.9 ± 0.4[k,n]	1.005 (da)	0.744	22.47[o]	71.2	AIST (9/12)	Sharp[20]
Dye (minimodule)	10.7 ± 0.4[k,n]	26.55 (da)	0.754[d]	20.19[d,p]	69.9	AIST (2/15)	Sharp, 7 serial cells[21]

(Continues)

TABLE 1 (Continued)

Classification	Efficiency, %	Area, cm^2	V_{oc}, V	J_{sc}, mA/cm^2	Fill Factor, %	Test Centre (Date)	Description
Dye (submodule)	8.8 ± 0.3[n]	398.8 (da)	0.697[d]	18.42[d,q]	68.7	AIST (9/12)	Sharp, 26 serial cells[22]
Organic							
Organic (cell)	11.2 ± 0.3[r]	0.992 (da)	0.780	19.30[e]	74.2	AIST (10/15)	Toshiba[23]
Organic (minimodule)	9.7 ± 0.3[r]	26.14 (da)	0.806[d]	16.47[d,p]	73.2	AIST (2/15)	Toshiba (8 series cells)[23]

Abbreviations: CIGS, $CuIn_{1-y}Ga_ySe_2$; a-Si, amorphous silicon/hydrogen alloy; nc-Si, nanocrystalline or microcrystalline silicon; CZTSSe, $Cu_2ZnSnS_{4-y}Se_y$; CZTS, Cu_2ZnSnS_4; (ap), aperture area; (t), total area; (da), designated illumination area; FhG-ISE, Fraunhofer Institut für Solare Energiesysteme; AIST, Japanese National Institute of Advanced Industrial Science and Technology.

[a]Spectral response and current-voltage curve reported in Version 50 of these tables.

[b]Not measured at an external laboratory.

[c]Spectral response and current-voltage curve reported in Version 51 of these tables.

[d]Reported on a “per cell” basis.

[e]Spectral responses and current-voltage curve reported in Version 45 of these tables.

[f]Recalibrated from original measurement.

[g]Spectral response and current-voltage curve reported in the Version 53 of these tables.

[h]Spectral response and current-voltage curve reported in the present version of these tables.

[i]Stabilised by 1000-h exposure to 1 sun light at 50 C.

[j]Initial performance. References 24 and 25 review the stability of similar devices.

[k]Average of forward and reverse sweeps at 150 mV/s (hysteresis ± 0.26%).

[l]Measured using 13-point IV sweep with constant bias until data constant at 0.05% level.

[m]Spectral response and current-voltage curve reported in Version 52 of these tables.

[n]Initial efficiency. Reference 26 reviews the stability of similar devices.

[o]Spectral response and current-voltage curve reported in Version 41 of these tables.

[p]Spectral response and current-voltage curve reported in Version 46 of these tables.

[q]Spectral response and current-voltage curve reported in Version 43 of these tables.

[r]Initial performance. References 27 and 28 review the stability of similar devices.

TABLE 2 "Notable exceptions" for single-junction cells and submodules: "Top dozen" confirmed results, not class records, measured under the global AM1.5 spectrum (1000 Wm^{-2}) at 25°C (IEC 60904-3: 2008, ASTM G-173-03 global)

Classification	Efficiency, %	Area, cm^2	V_{oc}, V	J_{sc}, mA/cm^2	Fill Factor, %	Test Centre (Date)	Description
Cells (silicon)							
Si (crystalline)	25.0 ± 0.5	4.00 (da)	0.706	42.7[a]	82.8	Sandia (3/99)[b]	UNSW p-type PERC top/rear contacts[29]
Si (crystalline)	25.8 ± 0.5[c]	4.008 (da)	0.7241	42.87[d]	83.1	FhG-ISE (7/17)	FhG-ISE, n-type top/rear contacts[30]
Si (crystalline)	26.1 ± 0.3[c]	3.9857 (da)	0.7266	42.62[e]	84.3	ISFH (2/18)	ISFH, p-type rear IBC[31]
Si (large crystalline)	**25.1 ± 0.5**	**151.88 (ap)**	**0.7375**	**40.79[f]**	**83.5**	**FhG-ISE (9/15)**	**Kaneka, n-type top/rear contacts[32]**
Si (large crystalline)	26.6 ± 0.5	179.74 (da)	0.7403	42.5[g]	84.7	FhG-ISE (11/16)	Kaneka, n-type rear IBC[4]
Si (multicrystalline)	22.0 ± 0.4	245.83 (t)	0.6717	40.55[d]	80.9	FhG-ISE (9/17)	Jinko Solar, large p-type[33]
Cells (III-V)							
GaInP	**22.0 ± 0.3[c]**	**0.2502 (ap)**	**1.4695**	**16.63[h]**	**90.2**	**NREL (1/19)**	**NREL, rear HJ, strained AlInP[34]**
Cells (chalcogenide)							
CdTe (thin-film)	22.1 ± 0.5	0.4798 (da)	0.8872	31.69[i]	78.5	Newport (11/15)	First Solar on glass[35]
CZTSSe (thin-film)	12.6 ± 0.3	0.4209 (ap)	0.5134	35.21[j]	69.8	Newport (7/13)	IBM solution grown[36]
CZTS (thin-film)	11.0 ± 0.2	0.2339(da)	0.7306	21.74[g]	69.3	NREL (3/17)	UNSW on glass[37]
Cells (other)							
Perovskite (thin film)	**24.2 ± 0.8[k,l]**	**0.0955 (ap)**	**1.1948**	**24.16[h]**	**84.0**	**Newport (1/19)**	**KRICT, Korea[38]**
Organic (thin film)	**16.4 ± 0.2[m]**	**0.04137 (da)**	**0.8468**	**25.46[h]**	**76.3**	**NREL (5/19)**	**SCUT, China[39]**
Organic (thin film)	**16.4 ± 0.4[m]**	**0.0394 (da)**	**0.8621**	**26.17[h]**	**72.7**	**Newport (5/19)**	**HKUST, Hong Kong[40]**

Abbreviations: CIGSSe, CuInGaSSe; CZTSSe, $Cu_2ZnSnS_{4-y}Se_y$; CZTS, Cu_2ZnSnS_4; (ap), aperture area; (t), total area; (da), designated illumination area; AIST, Japanese National Institute of Advanced Industrial Science and Technology; NREL, National Renewable Energy Laboratory; FhG-ISE, Fraunhofer-Institut für Solare Energiesysteme; ISFH, Institute for Solar Energy Research, Hamelin.

[a]Spectral response reported in Version 36 of these tables.

[b]Recalibrated from original measurement.

[c]Not measured at an external laboratory.

[d]Spectral response and current-voltage curves reported in Version 51 of these tables.

[e]Spectral response and current-voltage curve reported in Version 52 of these tables.

[f]Spectral response and current-voltage curves reported in Version 47 of these tables.

[g]Spectral response and current-voltage curves reported in Version 50 of these tables.

[h]Spectral response and current-voltage curve reported in the present version of these tables.

[i]Spectral response and/or current-voltage curves reported in Version 46 of these tables.

[j]Spectral response and current-voltage curves reported in Version 44 of these tables.

[k]Stability not investigated. References 24 and 25 document stability of similar devices.

[l]Measured using 13 point IV sweep with constant voltage bias until current determined as unchanging.

[m]Long-term stability not investigated. References 27 and 28 document stability of similar devices.

TABLE 3 Confirmed multiple-junction terrestrial cell and submodule efficiencies measured under the global AM1.5 spectrum (1000 W/m^2) at 25°C (IEC 60904-3: 2008, ASTM G-173-03 global)

Classification	Efficiency, %	Area, cm^2	Voc, V	Jsc, mA/cm^2	Fill Factor, %	Test Centre (Date)	Description
III-V multijunctions							
Five junction cell (bonded)	38.8 ± 1.2	1.021 (ap)	4.767	9.564	85.2	NREL (7/13)	Spectrolab, two terminal[41]
(2.17/1.68/1.40/1.06/.73 eV)							
InGaP/GaAs/InGaAs	37.9 ± 1.2	1.047 (ap)	3.065	14.27[a]	86.7	AIST (2/13)	Sharp, two term.[42]

(Continues)

TABLE 3 (Continued)

Classification	Efficiency, %	Area, cm^2	Voc, V	Jsc, mA/cm^2	Fill Factor, %	Test Centre (Date)	Description
GaInP/GaAs (monolithic)	32.8 ± 1.4	1.000 (ap)	2.568	14.56[b]	87.7	NREL (9/17)	LG Electronics, two term.
Multijunctions with c-Si							
GaInP/GaAs/Si (mech. Stack)	35.9 ± 0.5[c]	1.002 (da)	2.52/0.681	13.6/11.0	87.5/78.5	NREL (2/17)	NREL/CSEM/EPFL, four term.[43]
GaInP/GaAs/Si (wafer bonded)	33.3 ± 1.2[c]	3.984 (ap)	3.127[b]	12.7[b]	83.5	FhG-ISE (8/17)	Fraunhofer ISE, two term.[44]
GaInP/GaAs/Si (monolithic)	22.3 ± 0.8[c]	0.994 (ap)	2.619	10.0[d]	85.0	FhG-ISE (10/18)	Fraunhofer ISE, two term.[45]
GaAsP/Si (monolithic)	20.1 ± 1.3[c]	3.940 (ap)	1.673	14.94[e]	80.3	NREL (5/18)	OSU/SolAero/UNSW, two term.[46]
GaAs/Si (mech. Stack)	32.8 ± 0.5[c]	1.003 (da)	1.09/0.683	28.9/11.1[e]	85.0/79.2	NREL (12/16)	NREL/CSEM/EPFL, four term.[43]
Perovskite/Si (monolithic)	**28.0 ± 0.7[f]**	**1.030 (da)**	**1.802**	**19.75[g]**	**78.7**	**NREL (12/18)**	**Oxford PV[47]**
GaInP/GaInAs/Ge; Si (spectral split minimodule)	34.5 ± 2.0	27.83 (ap)	2.66/0.65	13.1/9.3	85.6/79.0	NREL (4/16)	UNSW/Azur/Trina, four term.[48]
a-Si/nc-Si multijunctions							
a-Si/nc-Si/nc-Si (thin-film)	14.0 ± 0.4[h,c]	1.045 (da)	1.922	9.94[i]	73.4	AIST (5/16)	AIST, two term.[49]
a-Si/nc-Si (thin-film cell)	12.7 ± 0.4[h,c]	1.000(da)	1.342	13.45[j]	70.2	AIST (10/14)	AIST, two term.[50]
"Notable exceptions"							
Perovskite/CIGS	22.4 ± 1.9[f]	0.042 (da)[k]	1.774	17.3[e]	73.1	NREL (11/17)	UCLA, two term.[51]
GaInP/GaAs/GaInAs	37.8 ± 1.4	0.998 (ap)	3.013	14.60[d]	85.8	NREL (1/18)	Microlink (ELO)[52]
Six junction (monolithic) (2.19/1.76/1.45/1.19/.97/.7 eV)	**39.2 ± 3.2[c]**	**0.247 (ap)[k]**	**5.549**	**8.457[g]**	**83.5**	**NREL (11/18)**	**NREL, inv. m'morphic[53]**

Abbreviations: a-Si, amorphous silicon/hydrogen alloy; nc-Si, nanocrystalline or microcrystalline silicon; (ap), aperture area; (t), total area; (da), designated illumination area; FhG-ISE, Fraunhofer Institut für Solare Energiesysteme; AIST, Japanese National Institute of Advanced Industrial Science and Technology.

[a]Spectral response and current-voltage curve reported in Version 42 of these Tables.

[b]Spectral response and current-voltage curve reported in the Version 51 of these tables.

[c]Not measured at an external laboratory.

[d]Spectral response and current-voltage curve reported in Version 53 of these tables.

[e]Spectral response and current-voltage curve reported in Version 52 of these tables.

[f]Initial efficiency. References 24 and 25 review the stability of similar perovskite-based devices.

[g]Spectral response and current-voltage curve reported in the present version of these tables.

[h]Stabilised by 1000-h exposure to 1 sun light at 50 C.

[i]Spectral response and current-voltage curve reported in Version 49 of these tables.

[j]Spectral responses and current-voltage curve reported in Version 45 of these tables.

[k]Area too small to qualify as outright class record.

TABLE 4 Confirmed terrestrial module efficiencies measured under the global AM1.5 spectrum (1000 W/m^2) at a cell temperature of 25°C (IEC 60904-3: 2008, ASTM G-173-03 global)

Classification	Effic., %	Area, cm^2	V_{oc}, V	I_{sc}, A	FF, %	Test Centre (Date)	Description
Si (crystalline)	24.4 ± 0.5	13177 (da)	79.5	5.04[a]	80.1	AIST (9/16)	Kaneka (108 cells)[4]
Si (multicrystalline)	19.9 ± 0.4	15143 (ap)	78.87	4.795[a]	79.5	FhG-ISE (10/16)	Trina Solar (120 cells)[54]
GaAs (thin film)	25.1 ± 0.8	866.45 (ap)	11.08	2.303[b]	85.3	**FhG-ISE** (11/17)	Alta Devices[55]
CIGS (Cd free)	19.2 ± 0.5	841 (ap)	48.0	0.456[b]	73.7	AIST (1/17)	Solar Frontier (70 cells)[56]
CdTe (thin film)	18.6 ± 0.5	7038.8 (da)	110.6	1.533[d]	74.2	NREL (4/15)	First Solar, monolithic[57]
a-Si/nc-Si (tandem)	12.3 ± 0.3[f]	14322 (t)	280.1	0.902[f]	69.9	ESTI (9/14)	TEL Solar, Trubbach Labs[58]
Perovskite	11.6 ± 0.4[g]	802 (da)	23.79	0.577[h]	68.0	AIST (4/18)	Toshiba (22 cells)[19]

(Continues)

TABLE 4 (Continued)

Classification	Effic., %	Area, cm^2	V_{oc}, V	I_{sc}, A	FF, %	Test Centre (Date)	Description
Organic	8.7 ± 0.3[h]	802 (da)	17.47	0.569[d]	70.4	AIST (5/14)	Toshiba[23]
Multijunction							
InGaP/GaAs/InGaAs	31.2 ± 1.2	968 (da)	23.95	1.506	83.6	AIST (2/16)	Sharp (32 cells)[59]
"Notable exception"							
CIGS (large)	**17.4 ± 0.6**	**10850 (ap)**	**58.20**	**4.379**[i]	**74.3**	**FhG-ISE (4/19)**	**Miasole**[60]

Abbreviations: CIGSS, CuInGaSSe; a-Si, amorphous silicon/hydrogen alloy; a-SiGe, amorphous silicon/germanium/hydrogen alloy; nc-Si, nanocrystalline or microcrystalline silicon; Effic., efficiency; (t), total area; (ap), aperture area; (da), designated illumination area; FF, fill factor.

[a]Spectral response and current voltage curve reported in Version 49 of these tables.

[b]Spectral response and current-voltage curve reported in Version 50 or 51 of these tables.

[c]Spectral response and/or current-voltage curve reported in Version 47 of these tables.

[d]Spectral response and current-voltage curve reported in Version 45 of these tables.

[e]Stabilised at the manufacturer to the 2% level following IEC procedure of repeated measurements.

[f]Spectral response and/or current-voltage curve reported in Version 46 of these tables.

[g]Initial performance. References 24 and 25 review the stability of similar devices.

[h]Spectral response and current-voltage curve reported in the present version of these tables.

[i]Spectral response reported in the present version of these tables.

entries based on their significance and timeliness. To encourage discrimination, the table is limited to nominally 12 entries with the present authors having voted for their preferences for inclusion. Readers who have suggestions of notable exceptions for inclusion into this or subsequent tables are welcome to contact any of the authors with full details. Suggestions conforming to the guidelines will be included on the voting list for a future issue.

Table 3 was first introduced in Version 49 of these tables and summarises the growing number of cell and submodule results involving high efficiency, one-sun multiple-junction devices (previously reported in Table 1). Table 4 shows the best results for one-sun modules, both single and multiple junction, while Table 5 shows the best results for concentrator cells and concentrator modules. A small number of "notable exceptions" are also included in Tables 3–5.

2 | NEW RESULTS

Ten new results are reported in the present version of these tables with one earlier result reinstated. The first new result in Table 1 ("one-sun cells") represents an outright record for any reasonably sized polycrystalline thin-film solar cell. An efficiency of 23.35% was measured for a 1-cm^2 CIGS ($CuIn_xGa_{1-x}S_ySe_{1-y}$) cell fabricated by Solar Frontier[11] and measured at the Japanese National Institute of Advanced Industrial Science and Technology (AIST). As with the commercial product marketed by Solar Frontier, this cell was Cd-free.

The first of five new results in Table 2 (one-sun "notable exceptions") is reinstatement of a result reported earlier in Version 47 of these tables. An efficiency of 25.1% was reported for a large 152-cm^2 n-type silicon cell fabricated by Kaneka (Osaka, Japan)[32] and confirmed by the Fraunhofer Institute for Solar Energy Systems (FhG-ISE). This efficiency is the highest reported for a large silicon cell with the two different polarity contacts on opposite front and rear cell surfaces and is reinstated to encourage competition in this commercially relevant space.

The second new result is a new efficiency record of 22.0% for a 0.25-cm^2 wide-bandgap GaInP cell with a rear heterojunction (HJ) and a strained AlInP layer. The cell was fabricated and measured by the National Renewable Energy Laboratory (NREL). It is the first cell reported in these tables with fill factor (FF) above 90%. Cell area is too small for classification as an outright record, with solar cell efficiency targets in governmental research programs generally specified in terms of a cell area of 1 cm^2 or larger.[61-63]

The third new result represents a new record for a Pb-halide perovskite solar cell, with an efficiency of 24.2% confirmed for a small area 0.1-cm^2 cell fabricated by the Korean Research Institute of Chemical Technology (KRICT)[38] and measured at the Newport PV Laboratory. Cell area is again too small for classification as an outright record.

For perovskite cells, the tables now accept results based on "quasi-steady-state" measurements (sometimes called "stabilised" in the perovskite field, although this conflicts with usage in other areas of photovoltaics). Along with other emerging technologies, perovskite cells may not demonstrate the same level of stability as conventional cells, with the stability of perovskite cells discussed elsewhere.[24,25]

The final new "notable exceptions" in Table 2 are for two very small area (0.04 cm^2) organic (OPV) solar cells fabricated by the Southern China University of Technology (SCUT)[39] and the Hong Kong University of Science and Technology (HKUST)[40] measured at NREL and at the Newport PV Laboratory, respectively. Both cells demonstrate an efficiency of 16.4% and continue the rapid rise in OPV efficiency noted in the previous version of these tables.[1] The stability of organic solar cells is discussed elsewhere[27,28] with cell area again too small for classification as an outright record.

TABLE 5 Terrestrial concentrator cell and module efficiencies measured under the ASTM G-173-03 direct beam AM1.5 spectrum at a cell temperature of 25°C

Classification	Effic., %	Area, cm^2	Intensity[a], suns	Test Centre (Date)	Description
Single cells					
GaAs	29.3 ± 0.7[b]	0.09359 (da)	49.9	NREL (10/16)	LG Electronics
Si	27.6 ± 1.2[c]	1.00 (da)	92	FhG-ISE (11/04)	Amonix back-contact[64]
CIGS (thin film)	23.3 ± 1.2[d,e]	0.09902 (ap)	15	NREL (3/14)	NREL[65]
Multijunction cells					
AlGaInP/AlGaAs/GaAs/GaInAs(3) (2.15/1.72/1.41/1.17/0.96/0.70 eV)	**47.1 ± 2.6**[d,f]	**0.099 (da)**	**143**	**NREL (3/19)**	**NREL, 6j inv. m'morphic**[53]
GaInP/GaAs/GaInAsP/GaInAs	46.0 ± 2.2[g]	0.0520 (da)	508	AIST (10/14)	Soitec/CEA/FhG-ISE 4j bonded[66]
GaInP/GaAs/GaInAs/GaInAs	45.7 ± 2.3[d,h]	0.09709 (da)	234	NREL (9/14)	NREL, 4j monolithic[67]
InGaP/GaAs/InGaAs	44.4 ± 2.6[i]	0.1652 (da)	302	FhG-ISE (4/13)	Sharp, 3j inverted metamorphic[68]
GaInAsP/GaInAs	35.5 ± 1.2[j,d]	0.10031 (da)	38	NREL (10/17)	NREL 2-junction (2j)
Minimodule					
GaInP/GaAs; GaInAsP/GaInAs	43.4 ± 2.4[d,k]	18.2 (ap)	340[l]	FhG-ISE (7/15)	Fraunhofer ISE 4j (lens/cell)[69]
Submodule					
GaInP/GaInAs/Ge; Si	40.6 ± 2.0[k]	287 (ap)	365	NREL (4/16)	UNSW 4j split spectrum[70]
Modules					
Si	20.5 ± 0.8[d]	1875 (ap)	79	Sandia (4/89)[m]	Sandia/UNSW/ENTECH (12 cells)[71]
Three junction (3j)	35.9 ± 1.8[n]	1092 (ap)	N/A	NREL (8/13)	Amonix[72]
Four junction (4j)	38.9 ± 2.5[o]	812.3 (ap)	333	FhG-ISE (4/15)	Soitec[73]
"Notable exceptions"					
Si (large area)	21.7 ± 0.7	20.0 (da)	11	Sandia (9/90)[k]	UNSW laser grooved[74]
Luminescent minimodule	7.1 ± 0.2	25(ap)	2.5[l]	ESTI (9/08)	ECN Petten, GaAs cells[75]

Abbreviations: CIGS, $CuInGaSe_2$, Effic., efficiency, (da), designated illumination area, (ap), aperture area, NREL, National Renewable Energy Laboratory, FhG-ISE, Fraunhofer-Institut für Solare Energiesysteme.

[a]One sun corresponds to direct irradiance of 1000 Wm^{-2}.

[b]Spectral response and current-voltage curve reported in Version 50 of these tables.

[c]Measured under a low aerosol optical depth spectrum similar to ASTM G-173-03 direct.[76]

[d]Not measured at an external laboratory.

[e]Spectral response and current-voltage curve reported in Version 44 of these tables.

[f]Spectral response and current-voltage curve reported in the present version of these tables.

[g]Spectral response and current-voltage curve reported in Version 45 of these tables.

[h]Spectral response and current-voltage curve reported in Version 46 of these tables.

[i]Spectral response and current-voltage curve reported in Version 42 of these tables.

[j]Spectral response and current-voltage curve reported in Version 51 of these tables.

[k]Determined at IEC 62670-1 CSTC reference conditions.

[l]Geometric concentration.

[m]Recalibrated from original measurement.

[n]Referenced to 1000 W/m^2 direct irradiance and 25°C cell temperature using the prevailing solar spectrum and an in-house procedure for temperature translation.

[o]Measured under IEC 62670-1 reference conditions following the current IEC power rating draft 62670-3.

Two new results are reported in Table 3 relating to one-sun, multijunction devices. The first is 28.0% for a 1-cm^2 perovskite/silicon monolithic two-junction, two-terminal device fabricated by Oxford PV[47] and again measured by NREL. Note that this efficiency now comfortably exceeds the highest efficiency for a single-junction silicon cell (Table 1), although for a much smaller area device.

A second new result for Table 3 is included as a multijunction cell "notable exception." An efficiency of 39.2% was measured for a 0.25-cm^2 six-junction, two-terminal, inverted metamorphic, monolithic $Al_{0.24}Ga_{0.26}In_{0.5}P/Al_{0.26}Ga_{0.74}As/Al_{0.03}Ga_{0.97}As/Ga_{0.86}In_{0.14}As/Ga_{0.68}In_{0.32}As/Ga_{0.43}In_{0.57}As$ cell fabricated by and measured at NREL.[53] This is the highest efficiency ever measured for a one-

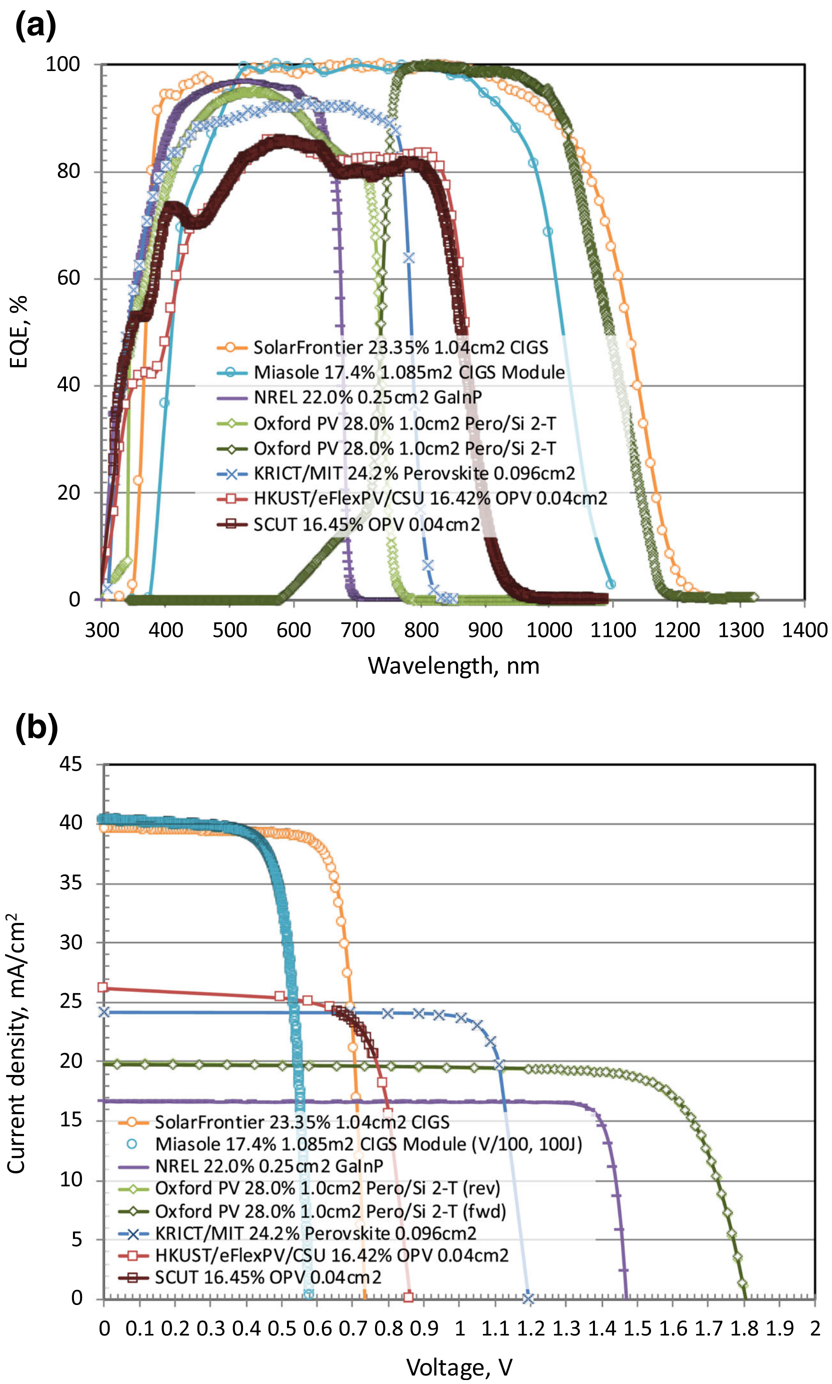

FIGURE 1 A, External quantum efficiency (EQE) for the new CIGS cell and module results, for the 28.0% perovskite/Si tandem cell result as well as for the new OPV, perovskite, and GaInP cell results reported in this issue (some results may be normalised); B, corresponding current density-voltage (JV) curves [Colour figure can be viewed at wileyonlinelibrary.com]

sun cell, although again cell area is too small to be considered as an outright record.

One new entry in Table 4 ("one-sun modules") as a "notable exception" is an efficiency of 17.4% for a large-area (1 m^2), flexible CIGS module fabricated by MiaSolé[60] and measured by FhG-ISE.

The final new entry is in Table 5 ("concentrator cells and modules") where an efficiency of 47.1% has been measured for a 0.1-cm^2 six-junction, two-terminal, inverted metamorphic, monolithic $Al_{0.23}$ $Ga_{0.27}$ $In_{0.5}$ P/$Al_{0.23}$ $Ga_{0.77}$ As / GaAs / $Ga_{0.84}$ $In_{0.16}$ As/$Ga_{0.67}$ $In_{0.33}$ As/$Ga_{0.43}$ $In_{0.57}$ As cell at 143-suns concentration (143-kW/m^2 irradiance), with the cell fabricated by and measured at NREL.[53] This is the highest efficiency ever reported for any photovoltaic cell, although concentrator cell efficiencies are not strictly thermodynamic efficiencies, because they exclude diffuse light on the system aperture in the efficiency determination.

The EQE spectra for the new CIGS cell and module results as well as for the 28.0% perovskite/Si tandem cell result and for the new OPV, perovskite, and GaInP cell results reported in the present issue of these tables are shown in Figure 1A, with Figure 1B showing the current density-voltage (JV) curves for the same devices. Figure 2A,B shows the corresponding EQE and JV curves for the new six-junction, two-terminal cell results.

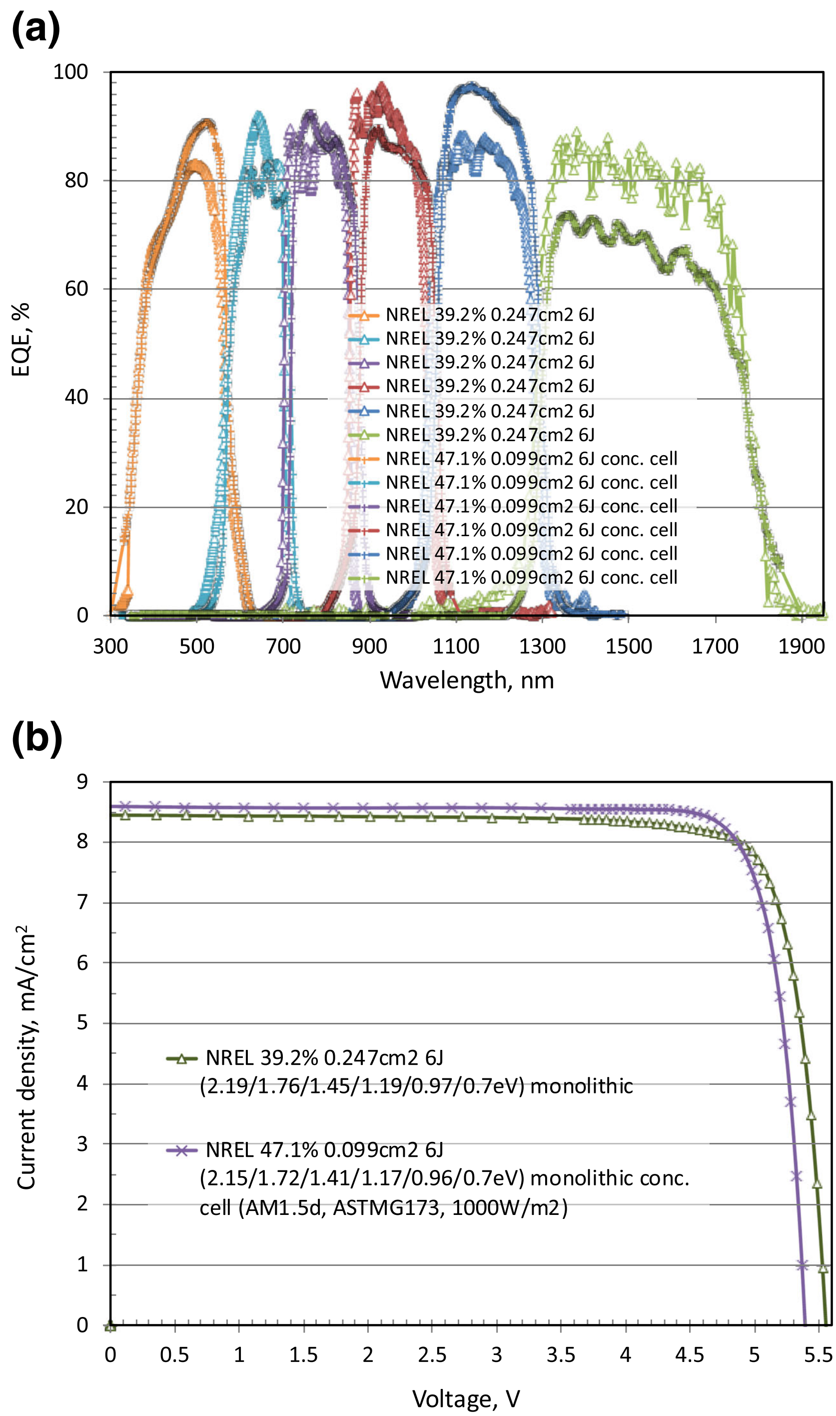

FIGURE 2 A, External quantum efficiency (EQE) for the new six-junction multijunction cell results reported in this issue (some results may be normalised); B, corresponding current density-voltage (JV) curves [Colour figure can be viewed at wileyonlinelibrary.com]

DISCLAIMER

While the information provided in the tables is provided in good faith, the authors, editors, and publishers cannot accept direct responsibility for any errors or omissions.

ACKNOWLEDGEMENT

The Australian Centre for Advanced Photovoltaics commenced operation in February 2013 with support from the Australian Government through the Australian Renewable Energy Agency (ARENA). The Australian Government does not accept responsibility for the views, information, or advice expressed herein. The work by D. Levi was supported by the US Department of Energy under Contract No. DE-AC36-08-GO28308 with the National Renewable Energy Laboratory. The work at AIST was supported in part by the Japanese New Energy and Industrial Technology Development Organisation (NEDO) under the Ministry of Economy, Trade and Industry (METI).

ORCID

Martin A. Green https://orcid.org/0000-0002-8860-396X
Anita W.Y. Ho-Baillie https://orcid.org/0000-0001-9849-4755

REFERENCES

1. Green MA, Hishikawa Y, Warta W, et al. Solar cell efficiency tables (version 53). *Prog Photovolt Res Appl*. 2019;27(1):3-12.
2. Green MA, Hishikawa Y, Warta W, et al. Solar cell efficiency tables (version 51). *Prog Photovolt Res Appl*. 2018;26(1):3-12.
3. Green MA, Emery K, Hishikawa Y, Warta W. Solar cell efficiency tables (version 33). *Prog Photovolt Res Appl*. 2009;17(1):85-94.
4. Yoshikawa K, Kawasaki H, Yoshida W, et al. Silicon heterojunction solar cell with interdigitated back contacts for a photoconversion efficiency over 26%. *Nat Energy*. 2017;2(5):17032.
5. Benick J, Richter A, Müller R, et al. High-efficiency n-type HP mc silicon solar cells. *IEEE J Photovolt*. 2017;7(5):1171-1175.
6. Moslehi MM, Kapur P, Kramer J, Rana V, Seutter S, Deshpande A, Stalcup T, Kommera S, Ashjaee J, Calcaterra A, Grupp D, Dutton D, Brown R. World-record 20.6% efficiency 156 mm x 156 mm full-square solar cells using low-cost kerfless ultrathin epitaxial silicon & porous silicon lift-off technology for industry-leading high-performance smart PV modules. PV Asia Pacific Conference (APVIA/PVAP), 24 October 2012.
7. Keevers MJ, Young TL, Schubert U, Green MA. 10% efficient CSG minimodules. *22nd European Photovoltaic Solar Energy Conference*, Milan, September 2007.
8. Kayes BM, Nie H, Twist R, Spruytte SG, Reinhardt F, Kizilyalli IC, Higashi GS. 27.6% conversion efficiency, a new record for single-junction solar cells under 1 sun illumination. Proceedings of the 37th IEEE Photovoltaic Specialists Conference, 2011.
9. Venkatasubramanian R, O'Quinn BC, Hills JS, Sharps PR, Timmons ML, Hutchby JA, Field H, Ahrenkiel A, Keyes B. 18.2% (AM1.5) efficient GaAs solar cell on optical-grade polycrystalline Ge substrate. *Conference Record*, 25th IEEE Photovoltaic Specialists Conference, Washington, May 1997, 31–36.
10. Wanlass M. Systems and methods for advanced ultra-high-performance InP solar cells. US Patent 9,590,131 B2, 7 March 2017.
11. Nakamura M, Yamaguchi K, Kimoto Y, Yasaki Y, Kato T, Sugimoto H. Cd-free Cu (In,Ga)(Se,S)2 thin-film solar cell with a new world record efficacy of 23.35%, 46th IEEE PVSC, Chicago, IL, June 19, 2019 (see also http://www.solar-frontier.com/eng/news/2019/0117_press.html)
12. First Solar Press Release, First Solar builds the highest efficiency thin film PV cell on record, 5 August 2014.
13. https://en.dgist.ac.kr/site/dgist_eng/menu/984.do (accessed 28/10/2018).
14. Yan C, Huang J, Sun K, et al. Cu_2ZnSn S_4 solar cells with over 10% power conversion efficiency enabled by heterojunction heat treatment. *Nat Energy*. 2018;3(9):764-772.
15. Matsui T, Bidiville A, Sai H, et al. High-efficiency amorphous silicon solar cells: impact of deposition rate on metastability. *Appl Phys Lett*. 2015;106(5):053901. https://doi.org/10.1063/1.4907001
16. Sai H, Maejima K, Matsui T, et al. High-efficiency microcrystalline silicon solar cells on honeycomb textured substrates grown with high-rate VHF plasma-enhanced chemical vapor deposition. *Jpn J Appl Phys*. 2015;54(8S1):08KB05.
17. Yang WS, Noh JH, Jeon NJ, et al. High-performance photovoltaic perovskite layers fabricated through intramolecular exchange. *Science*. 2015;348(6240):1234-1237.
18. http://www.microquanta.com (accessed 9 May, 2018).
19. Toshiba news release dated 25 September 2017 (https://www.toshiba.co.jp/rdc/rd/detail_e/e1709_02.html).
20. Komiya R, Fukui A, Murofushi N, Koide N, Yamanaka R and Katayama H. Improvement of the conversion efficiency of a monolithic type dye-sensitized solar cell module. *Technical Digest*, *21st International Photovoltaic Science and Engineering Conference*, Fukuoka, November 2011; 2C-5O-08.
21. Kawai M. High-durability dye improves efficiency of dye-sensitized solar cells. *Nikkei Electr*. 2013; Feb.1. http://techon.nikkeibp.co.jp/english/NEWS_EN/20130131/263532/ accessed 23 October, 2013
22. Mori S, Oh-oka H, Nakao H, et al. Organic photovoltaic module development with inverted device structure. *MRS Proc*. 2015;1737. https://doi.org/10.1557/opl.2015.540
23. Hosoya M, Oooka H, Nakao H, Gotanda T, Mori S, Shida N, Hayase R, Nakano Y, Saito M. Organic thin film photovoltaic modules. Proceedings of the 93rd Annual Meeting of the Chemical Society of Japan 2013; 21–37.
24. Han Y, Meyer S, Dkhissi Y, et al. Degradation observations of encapsulated planar $CH_3NH_3PbI_3$ perovskite solar cells at high temperatures and humidity. *J Mater Chem A*. 2015;3(15):8139-8147.
25. Yang Y, You J. Make perovskite solar cells stable. *Nature*. 2017; 544(7649):155-156.
26. Tanenbaum DM, Hermenau M, Voroshazi E, et al. The ISOS-3 inter-laboratory collaboration focused on the stability of a variety of organic photovoltaic devices. *RSC Adv*. 2012;2(3):882-893.
27. Krebs FC (Ed). *Stability and Degradation of Organic and Polymer Solar Cells*. Chichester: Wiley; 2012 Jorgensen M, Norrman K, Gevorgyan SA, Tromholt T, Andreasen B, Krebs FC. Stability of polymer solar cells. Advanced Materials 2012; 24**:** 580–612.
28. Krašovec UO, Bokalič M, Topič M. Ageing of DSSC studied by electroluminescence and transmission imaging. *Sol Energy Mater Sol Cells*. 2013;117:67-72.
29. Zhao J, Wang A, Green MA, Ferrazza F. Novel 19.8% efficient "honeycomb" textured multicrystalline and 24.4% monocrystalline silicon solar cells. *Appl Phys Lett*. 1998;73(14):1991-1993.
30. Richter A, Benick J, Feldmann F, Fell A, Hermle M, Glunz SW. N-type Si solar cells with passivating electron contact: identifying sources for efficiency limitations by wafer thickness and resistivity variation. *Sol Energy Mater Sol Cells*. 2017;173:96-105.
31. Haase F, Klamt C, Schäfer S, et al. Laser contact openings for local poly-Si-metal contacts enabling 26.1%-efficient POLO-IBC solar cells. *Sol Energy Mater Sol Cells*. 2018;186:184-193.
32. Yamamoto K, 25.1% efficiency Cu metallized heterojunction crystalline Si solar cell. 25th International Photovoltaic Science and Engineering Conference, Busan, Korea, November 2015.
33. https://www.jinkosolar.com/press_detail_1380.htm (accessed 9 May, 2018).
34. NREL, private communication, 22 May 2019.
35. First Solar Press Release. First Solar achieves yet another cell conversion efficiency world record, 24 February 2016.
36. Wang W, Winkler MT, Gunawan O, et al. Device characteristics of CZTSSe thin-film solar cells with 12.6% efficiency. *Adv Energy Mater*. 2013;4(7). https://doi.org/10.1002/aenm.201301465
37. Sun K, Yan C, Liu F, et al. Beyond 9% efficient kesterite Cu_2ZnSnS_4 solar cell: fabricated by using $Zn_{1-x}Cd_xS$ buffer layer. *Adv Energy Mater*. 2016;6(12):1600046. https://doi.org/10.1002/aenm.201600046
38. Jung EH, Jeon NJ, Park EY, et al. Efficient, stable and scalable perovskite solar cells using poly(3-hexylthiophene). *Nature*. 2019;567(7749):511-515.
39. Dong S, Zhang K, Xie BM, et al. High-performance large-area organic solar cells enabled by sequential bilayer processing via nonhalogenated solvents. *Adv Energy Mater*. 2019;9(1):1802832.

40. Zhang GG, Zhao JB, Chow PCY, et al. Nonfullerene acceptor molecules for bulk heterojunction organic solar cells. *Chem Rev*. 2018;118(7):3447-3507.

41. Chiu PT, Law DL, Woo RL, Singer S, Bhusari D, Hong WD, Zakaria A, Boisvert JC, Mesropian S, King RR, Karam NH. 35.8% space and 38.8% terrestrial 5J direct bonded cells. *Proc. 40th IEEE Photovoltaic Specialist Conference*, Denver, June 2014; 11–13.

42. Sasaki K, Agui T, Nakaido K, Takahashi N, Onitsuka R, Takamoto T. Proceedings, 9th International Conference on Concentrating Photovoltaics Systems, Miyazaki, Japan 2013.

43. Essig S, Allebé C, Remo T, et al. Raising the one-sun conversion efficiency of III–V/Si solar cells to 32.8% for two junctions and 35.9% for three junctions. *Nat Energy*. 2017;2(9):17144. https://doi.org/10.1038/nenergy.2017.144

44. Cariou R, Benick J, Feldmann F, et al. III-V-on-silicon solar cells reaching 33% photoconversion efficiency in two-terminal configuration. *Nat Energy*. 2018;3(4):326-333. https://doi.org/10.1038/s41560-018-0125-0

45. Feifel M, Ohlmann J, Benick J, et al. Direct growth of III-V/silicon triple-junction solar cells with 19.7% efficiency. *IEEE J Photovolt*. 2018;8(6):1590-1595.

46. Grassman TJ, Chmielewski DJ, Carnevale SD, Carlin JA, Ringel SA. $GaAs_{0.75}P_{0.25}$/Si dual-junction solar cells grown by MBE and MOCVD. *IEEE J Photovolt*. 2016;6(1):326-331.

47. https://www.oxfordpv.com/news/oxford-pv-perovskite-solar-cell-achieves-28-efficiency (accessed 22/5/2019).

48. Green MA, Keevers MJ, Concha Ramon B, Jiang Y, Thomas I, Lasich JB, Verlinden, PJ, Yang Y, Zhang X, Emery K, Moriarty T, King RR, Bensch W. Improvements in sunlight to electricity conversion efficiency: above 40% for direct sunlight and over 30% for global. Paper 1AP.1.2, *European Photovoltaic Solar Energy Conference* 2015, Hamburg, September 2015.

49. Sai H, Matsui T, Koida T, Matsubara K. Stabilized 14.0%-efficient triple-junction thin-film silicon solar cell. *Appl Phys Lett*. 2016;109:183506. https://doi.org/10.1063/1.49669986

50. Matsui T, Maejima K, Bidiville A, et al. High-efficiency thin-film silicon solar cells realized by integrating stable a-Si:H absorbers into improved device design. *Jpn J Appl Phys*. 2015;54(8S1):08KB10. https://doi.org/10.7567/JJAP.54.08KB10

51. http://yylab.seas.ucla.edu

52. http://mldevices.com/index.php/news/ (accessed 28/10/2018).

53. Geisz JF, Steiner MA, Jain N, et al. Building a six-junction inverted metamorphic concentrator solar cell. *IEEE J Photovolt*. 2018;8(2):626-632.

54. Verlinden PJ. Will we have >22% efficient multi-crystalline silicon solar cells? *PVSEC*. October, 2016;26, Singapore:24-28.

55. Mattos LS, Scully SR, Syfu M, Olson E, Yang L, Ling C, Kayes BM, He G. New module efficiency record: 23.5% under 1-sun illumination using thin-film single-junction GaAs solar cells. Proceedings of the 38th IEEE Photovoltaic Specialists Conference, 2012.

56. Sugimoto H. High efficiency and large volume production of CIS-based modules. *40th IEEE Photovoltaic Specialists Conference*, Denver, June 2014.

57. First Solar Press Release. First Solar achieves world record 18.6% thin film module conversion efficiency, 15 June 2015.

58. Cashmore JS, Apolloni M, Braga A, et al. Improved conversion efficiencies of thin-film silicon tandem (MICROMORPH ™) photovoltaic modules. *Sol Energy Mater Sol Cells*. 2016;144:84-95. https://doi.org/10.1016/j.solmat.2015.08.022

59. Takamoto, T. Application of InGaP/GaAs/InGaAs triple junction solar cells to space use and concentrator photovoltaic. *40th IEEE Photovoltaic Specialists Conference*, Denver, June 2014.

60. Bheemreddy V, Liu BJJ, Wills A, Murcia CP. Life prediction model development for flexible photovoltaic modules using accelerated damp heat testing. IEEE 7th World Conference on Photovoltaic Energy Conversion (WCPEC) 2018: 1249–1251.

61. Program milestones and decision points for single junction thin films. *Annual Progress Report* 1984, Photovoltaics, Solar Energy Research Institute, *Report* DOE/CE-0128, June 1985, **7**.

62. Sakata I, Tanaka Y, Koizawa K. Japan's New National R&D Program for Photovoltaics. *Photovoltaic Energy Conversion*, Conference Record of the 2006 IEEE 4th World Conference, Vol. 1, May 2008, 1–4.

63. Jäger-Waldau, A (Ed.). PVNET: *European Roadmap for PV R&D*, EUR 21087 EN, 2004.

64. Slade A, Garboushian V. 27.6% efficient silicon concentrator cell for mass production. *Technical Digest*, 15th International Photovoltaic Science and Engineering Conference, Shanghai, October 2005, 701.

65. Ward JS, Ramanathan K, Hasoon FS, et al. A 21.5% efficient Cu (In,Ga) Se2 thin-film concentrator solar cell. *Prog Photovolt Res Appl*. 2002;10(1):41-46.

66. Dimroth F, Tibbits TND, Niemeyer M, et al. Four-junction wafer-bonded concentrator solar cells. *IEEE J Photovolt*. January 2016;6(1):343-349. https://doi.org/10.1109/JPHOTOV.2015.2501729

67. NREL Press Release NR-4514, 16 December 2014.

68. Press Release, Sharp Corporation, 31 May 2012 (accessed at http://sharp-world.com/corporate/news/120531.html on 5 June 2013).

69. Steiner M, Siefer G, Schmidt T, Wiesenfarth M, Dimroth F, Bett AW. 43% sunlight to electricity conversion efficiency using CPV. *IEEE J Photovolt*. July 2016;6(4):1020-1024. https://doi.org/10.1109/JPHOTOV.2016.2551460

70. Green MA, Keevers MJ, Thomas I, Lasich JB, Emery K, King RR. 40% efficient sunlight to electricity conversion. *Prog Photovolt Res Appl*. 2015;23(6):685-691.

71. Chiang CJ and Richards EH. A 20% efficient photovoltaic concentrator module. *Conf. Record, 21st IEEE Photovoltaic Specialists Conference*, Kissimimee, May 1990: 861–863.

72. http://amonix.com/pressreleases/amonix-achieves-world-record-359-module-efficiency-rating-nrel-4 (accessed 23 October 2013).

73. van Riesen S, Neubauer M, Boos A, Rico MM, Gourdel C, Wanka S, Krause R, Guernard P, Gombert A. New module design with 4-junction solar cells for high efficiencies. Proceedings of the 11th Conference on Concentrator Photovoltaic Systems, 2015.

74. Zhang F, Wenham SR, Green MA. Large area, concentrator buried contact solar cells. *IEEE Trans Electron Devices*. 1995;42(1):144-149.

75. Slooff LH, Bende EE, Burgers AR, et al. A luminescent solar concentrator with 7.1% power conversion efficiency. *Phys Stat Sol (RRL)*. 2008;2(6):257-259.

76. Gueymard CA, Myers D, Emery K. Proposed reference irradiance spectra for solar energy systems testing. *Sol Energy*. 2002;73(6):443-467.

How to cite this article: Green MA, Dunlop ED, Levi DH, Hohl-Ebinger J, Yoshita M, Ho-Baillie AWY. Solar cell efficiency tables (version 54). *Prog Photovolt Res Appl*. 2019;27:565–575. https://doi.org/10.1002/pip.3171